Small-Scale Variability in Sea Surface Salinity and Implications for Satellite-Derived Measurements

NADYA T. VINOGRADOVA AND RUI M. PONTE

Atmospheric and Environmental Research, Inc., Lexington, Massachusetts

(Manuscript received 20 May 2013, in final form 14 August 2013)

ABSTRACT

Calibration and validation efforts of the *Aquarius* and *Soil Moisture and Ocean Salinity* (*SMOS*) satellite missions involve comparisons of satellite and in situ measurements of sea surface salinity (SSS). Such estimates of SSS can differ by the presence of small-scale variability, which can affect the in situ point measurement, but be averaged out in the satellite retrievals because of their large footprint. This study quantifies how much of a difference is expected between in situ and satellite SSS measurements on the basis of their different sampling of spatial variability. Maps of sampling error resulting from small-scale noise, defined here as the root-mean-square difference between ''local'' and footprint-averaged SSS estimates, are derived using a solution from a global high-resolution ocean data assimilation system. The errors are mostly <0.1 psu (global median is 0.05 psu), but they can be >0.2 psu in several regions, particularly near strong currents and outflows of major rivers. To examine small-scale noise in the context of other errors, its values are compared with the overall expected differences between monthly *Aquarius* SSS and Argo-based estimates. Results indicate that in several ocean regions, small-scale variability can be an important source of sampling error for the in situ measurements.

1. Introduction

An important component of the calibration and validation effort of any satellite mission is the comparison between remotely sensed and in situ measurements. For the recently launched *Aquarius/Satelite de Aplicaciones Cientificas-D* (*SAC-D*; Lagerloef et al. 2008; Lagerloef 2012) and *Soil Moisture and Ocean Salinity* (*SMOS*; Font et al. 2010) satellite missions dedicated to measuring sea surface salinity (SSS), comparison between retrieved and in situ observations is crucial in calibrating brightness temperatures of L-band radiometer and adjusting radiative transfer models necessary to derive SSS values (Le Vine et al. 2007).

One of the challenges in collocating the satellite and in situ data is the mismatch in their spatial coverage. While a measurement from in situ platforms, such as Argo floats, moored and drifting buoys, CTD, expendable CTD (XCTD), etc., provides a local SSS estimate, a single satellite retrieval represents a horizontal average over the sensor's footprint. Thus, variability on short horizontal scales—that is, shorter than the footprint (~150 km for *Aquarius*)—can contribute to differences between the satellite and in situ measurements. These small-scale features in SSS are typically associated with horizontal fronts and eddies, and can be important in several ocean regions (e.g., Delcroix et al. 2005; Hénin and Grelet 1996).

The objectives of this study are to examine how much variability is contained at small spatial scales (<1°) and to estimate a sampling error related to short-scale ''noise'' in a single, local SSS measurement. A 1° spacing is chosen to be comparable to typical *Aquarius* spatial resolution of approximately 150 km. It is also the horizontal resolution of the *Aquarius* level 3 salinity maps. The 1° analysis is also representative of the *Aquarius* level 2 beam footprints with dimensions of 76 km × 94 km, 84 km × 120 km, and 96 km × 156 km. The sampling error here is defined in terms of the ability of a single measurement within a 1° × 1° box to represent the true horizontal mean over this area, given the spatial variability of SSS fields. Defined in such way, the sampling error provides a measure of uncertainty of a single in situ measurement when comparing it to the *Aquarius* footprint averages and can be useful in satellite calibration/validation efforts. It can also provide

Corresponding author address: Nadya Vinogradova, AER Inc., 131 Hartwell Ave., Lexington, MA 02421.
E-mail: nadya@aer.com

DOI: 10.1175/JTECH-D-13-00110.1

a lower bound on the difference between the satellite and local estimates of SSS.

Previous work by Lagerloef and Delcroix (2001), Delcroix et al. (2005), and Lagerloef et al. (2010) discussed potential sampling errors in the planned *Aquarius* mission associated with small-scale SSS signals. By calculating the standard deviations of 2° samples in ship transects in the tropical Pacific Ocean, Lagerloef and Delcroix (2001, p. 147) concluded that the sampling error is generally less than 0.1 psu, though it can approach 0.3 psu in the presence of ''unusually strong SSS gradients.'' A more recent study by Lagerloef et al. (2010) examined the effect of spatial averaging of the SSS data from thermosalinograph sensors (TSG) by applying a 150-km-wide Gaussian filter along the ship tracks. They found that the root-mean-square difference between the high-resolution and spatially averaged along-track values is <0.1 psu, except in the Gulf Stream region, where it can be in the range 0.3–1 psu. To extend previous analyses, here we examine the effect of averaging resulting from the satellite footprint using the output of a high-resolution ocean model. The results are presented as a global assessment and are discussed in the context of the *Aquarius* calibration/validation efforts.

2. Methods

To examine the small-scale variability in SSS, denoted as σ_{sm}, we analyze a solution from the global high-resolution ($^1/_{12}°$) Hybrid Coordinate Ocean Model (HYCOM) constrained to a variety of ocean datasets through an assimilation scheme described by Chassignet et al. (2009). Thus, our proxy for a ''local measurement'' is HYCOM salinity representing an average over the grid cell, which is about 9 km near the equator and about 7 km on average at higher latitudes. HYCOM is an operational system and provides near real-time estimates of the ocean state. The system assimilates both surface observations, such as satellite altimetry and sea surface temperature, and vertical profiles of temperature and salinity, using the U.S. Navy Coupled Ocean Data Assimilation (NCODA) system (Cummings 2005). Vertical profiles of temperature and salinity are derived from either sea surface height anomalies through the Modular Ocean Data Assimilation System (MODAS; Fox et al. 2002), or from in situ measurements (Argo floats, XBTs, buoys). The solution is routinely validated (http://www7320.nrlssc.navy.mil/GLBhycom1-12/skill.html) and permits a good assessment of σ_{sm} in the presence of eddies and other short-scale features, such as fronts, instabilities, filaments, and rings that can be ''seen'' on a $^1/_{12}°$ grid. HYCOM is also a model of choice in the *Aquarius* simulation and validation efforts.

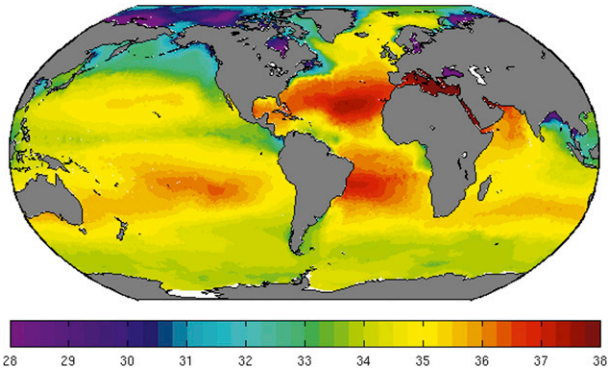

FIG. 1. Annual-mean SSS computed based on high-resolution ($^1/_{12}°$) HYCOM SSS fields during a 1-yr period of the *Aquarius* data collection from 25 Aug 2011 to 25 Aug 2012.

For our purposes, we use one year of daily-averaged salinity fields from the most recent HYCOM configuration (GLBa0.08/expt_90.9). The output is provided by the Center for Ocean–Atmospheric Prediction Studies (COAPS) at Florida State University and includes wintertime SSS values in high latitudes under ice-free conditions. The time period is chosen to coincide with the *Aquarius* data collection and runs from 25 August 2011 to 25 August 2012. Time scales resolved in the analyses involve periods longer than two days and include the seasonal cycle. HYCOM SSS fields represent an average over the top 1 m of its original vertical grid (isopycnal in the stratified open ocean, sigma coordinate in shallow coastal oceans, and fixed pressure levels in the surface mixed layer or nonstratified seas). Before analyses, HYCOM output is regridded from the curvilinear grid to a regular latitude–longitude grid following the procedure described in Vinogradova and Ponte (2012). As an example, Fig. 1 shows the time mean HYCOM SSS computed from daily high-resolution SSS fields over the period of interest. Relevant for our purposes, regions of strong salinity gradients are reproduced in the HYCOM solution, including western boundary currents, such as the Gulf Stream and Kuroshio, near the outflows of major rivers, such as the Amazon and Congo, coastal areas of the Bay of Bengal, the eastern Pacific fresh pool, etc. Details on the HYCOM performance and system validation can be found in Metzger et al. (2008a,b).

To approximate the large footprint of the *Aquarius* beams, HYCOM daily salinity values were averaged from the original $^1/_{12}°$ onto a 1° grid. The resulting averages ($\mathcal{S}$) are meant to represent salinity values as seen by the satellite over $1° \times 1°$ boxes. The standard deviation from $\mathcal{S}$ within each box provides a measure of the small-scale variability σ_{sm}. The values of σ_{sm} are computed for each box and for every day of the year.

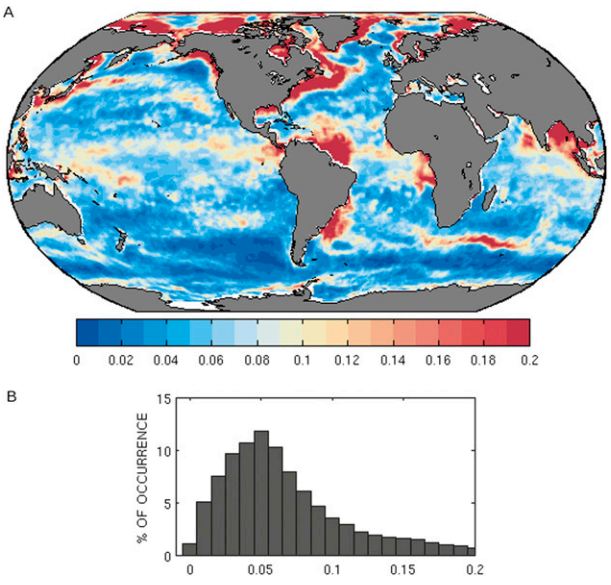

FIG. 2. (a) Sampling root-mean-square error ε_{sm} due to unresolved small-scale variability computed based on high-resolution, daily HYCOM SSS fields during the same 1-yr period as in Fig. 1. Values of ε_{sm} indicate how a single *Aquarius* measurement, approximated by the HYCOM SSS, can differ from local in situ measurement in the presence of short-scale noise. Notice that the color bar saturates at 0.2, while the values of ε_{sm} can reach a few salinity units (e.g., Gulf Stream region, Bay of Bengal, off the Amazon River basin, and Arctic Ocean) (b) Histogram of the average salinity difference resulting from small-scale variability computed based on the data from (a). The tail of the histogram is cut at 0.2.

The root-mean-square of all σ_{sm} defines the mean expected difference between the ''local'' and footprint-average salinity, or an average sampling error resulting from the small-scale noise, and is denoted as ε_{sm}.

3. Sampling errors resulting from small-scale noise

From Fig. 2a, the largest values of ε_{sm} are found in the regions of strong horizontal salinity gradients, including many coastal regions such as around Greenland and the Arctic, Gulf of Alaska, Gulf of Mexico, etc., where ε_{sm} can reach 1 psu. Large ε_{sm}, exceeding 0.2 psu, are also found near the outflows of major rivers, such as the Amazon and Congo Rivers, the Bay of Bengal region, and along strong currents like the Gulf Stream, Kuroshio, and Agulhas, which are characterized by the presence of energetic eddies and strong gradients in SSS and other surface properties, such as sea surface temperature (SST), sea level, and chlorophyll-*a*. In fact, sampling errors in SST related to small-scale variability inside $1° \times 1°$ boxes have patterns that are similar to those in Fig. 2a, particularly in the regions of strong currents [cf. Fig. 2 in Kaplan (2009) showing estimates of the spatial variability in SST inside a 1° bin computed based on the 4-km Pathfinder SST fields]. Values for ε_{sm} of approximately 0.1 psu are observed near the intertropical convergence zone (ITCZ) in both the North Atlantic and North Pacific Oceans, and the South Pacific convergence zone (SPCZ), among other regions. Tropical ε_{sm} values of 0.1 psu are consistent with those reported by Lagerloef and Delcroix (2001) and Delcroix et al. (2005) based on their analysis of SSS measurements from the thermosalinograph network. It is worth noting that while ε_{sm} represent an ''average'' measure of small-scale noise, σ_{sm} values show some seasonality, as well as variations at higher frequencies.

The estimated ε_{sm} values roughly follow a lognormal distribution with a median around 0.05 psu (Fig. 2b). The positive skew of the distribution implies that the mean is larger than the median. In this case, the global-mean value of ε_{sm} is approximately 0.1 psu, which is clearly affected by extreme values that can be as large as several practical salinity units. However, such instances are rare and 95% of the ε_{sm} values are <0.2 psu. Estimates in Fig. 2b closely follow the histogram based on a similar analysis of TSG data by Lagerloef et al. (2010; see also http://depts.washington.edu/papers/aquarius/presentations.html), who demonstrate that difference error between a point measurement and the area average over the satellite footprint fits a lognormal distribution with median around 0.05 psu. The similarity in error statistics between the analysis based on in situ measurements and the HYCOM solution lends confidence to the results in Fig. 2a, which, compared to previous studies, provides a more detailed map and larger coverage of sampling error associated with small-scale variability.

Values of ε_{sm} in Fig. 2a can be considered as an additional source of observational uncertainty to be applied to daily in situ measurements when comparing them with the *Aquarius* level 2 (or level 3) daily retrievals. For most local observations, measurement error is typically small. For example, measurement error for calibrated in situ salinity data is <0.01 psu. Sampling errors, as estimated in Fig. 2a, typically are larger. In our investigation, in regions where $\varepsilon_{sm} \gg 0.01$ psu, sampling error becomes the only important in situ error source and should be taken into account. In practice, one should add the value of ε_{sm} in the root-sum-square sense to the measurement error, if it is known, in order to define the lower bound for the expected difference between the daily satellite and in situ values. When comparing monthly averages (e.g., level 3 monthly products), the values of ε_{sm} should be scaled by $\sqrt{n_{obs}}$, where n_{obs} is the number of independent daily samples per month (e.g., Emery and Thomson 2004), which can depend on temporal and spatial decorrelation scales, etc.

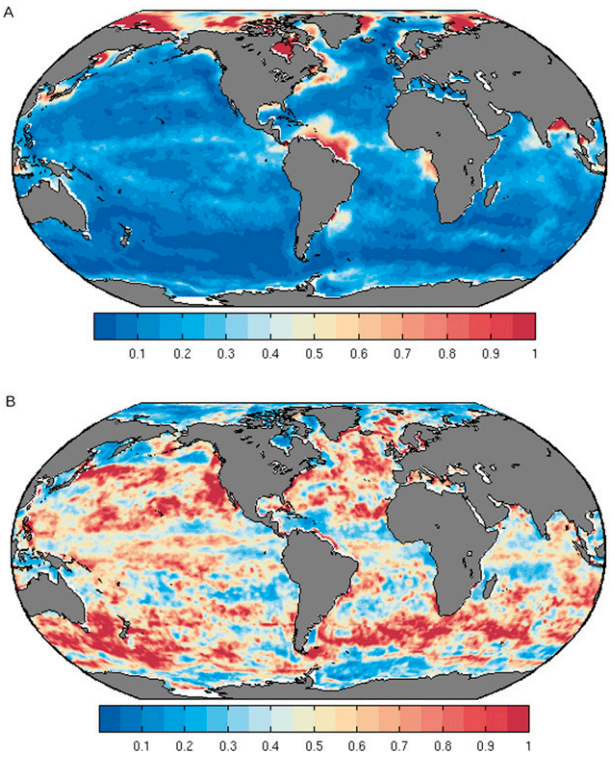

FIG. 3. (a) Standard deviation σ_t of HYCOM surface salinity fields computed based on 1-yr-long daily time series interpolated onto a 1° grid and describing variability in salinity at periods longer than two days, including seasonal cycle at scales captured by *Aquarius*. (b) Impact of short-scale noise defined as a ratio $r = \varepsilon_{sm}/\sigma_t$. Large ratio values indicate the potential regions where short-scale noise can affect the inference of temporal variability in salinity.

To further assess the importance of the estimated small-scale noise, it is useful to examine ε_{sm} in terms of the temporal variability in $\mathcal{S}$. Variability in $\mathcal{S}$, computed as the standard deviation over a 1-yr period, denoted as σ_t and shown in Fig. 3a, has typical values of around 0.1–0.2 psu, with maximum variability >1 psu. Notice that regions with large σ_t are often those where the impact of σ_{sm} is most significant, including the Bay of Bengal, off river mouths, and western boundary current regions (cf. Fig. 2a and Fig. 3a). This suggests that surface salinity in these regions is highly variable both in time and in space.

The ratio $r = \varepsilon_{sm}/\sigma_t$ can be used as an indicator of where the small-scale error might affect the inference of salinity variability. From Fig. 3b, the average of value of r is approximately 0.5. Values of $r > 0.5$ are seen in extensive regions at all latitudes, indicating that small-scale noise could measurably affect the inference of temporal variability in $\mathcal{S}$ from *Aquarius* retrievals, if not properly accounted for in calibration and validation procedures. For example, the impact of short-scale noise can be noticeable in boundary current regions, where ε_{sm} is large, as well as in stable subtropical regions, where σ_t is small and comparable to ε_{sm}. Recall that σ_t in Fig. 3a describes variations from 2 days to one year, and although it does include seasonal cycle, it does not include variations at very short (<2 days) or very long (interannual) time scales.

4. Small-scale noise and *Aquarius* validation

To improve calibration and validation process, it is useful to relate the magnitude of ε_{sm} to the overall differences between the satellite and in situ observations. As an example of the expected difference between the two estimates, we compare *Aquarius* measurements with in situ estimates based on Argo profiles. Argo-based estimates are used as monthly gridded (1°) salinity fields that are produced by the International Pacific Research Center (IPRC) using variational interpolation (http://apdrc.soest.hawaii.edu/). For the satellite retrievals we use *Aquarius* monthly level 3, version 2.0 reprocessed data, which are the current baseline algorithm in the *Aquarius* data processing stream. The data are provided by the Physical Oceanography Distributed Active Archive Center (PO.DAAC; http://podaac.jpl.nasa.gov/SeaSurfaceSalinity/Aquarius). Here we choose not to include *Aquarius* SSS values that are sampled during high-wind events ($>20\,m\,s^{-1}$), to avoid residual noise related to the removal of surface roughness effects (e.g., Lagerloef et al. 2013). Low SST conditions is another factor affecting *Aquarius* retrievals, leading to reduction in accuracy and positive bias compared to Argo (Boutin et al. 2013) and model simulations (Ebuchi and Abe 2012). For these reasons, regions in the Southern Ocean (southward of 45°S) are not examined.

We compute the difference between the monthly fields from the *Aquarius* and uppermost (typically 5 m) Argo estimates during the period of interest. The root-mean-square of all differences ε_{rms} has a global-mean value of around 0.3, with the highest values reaching up to a few practical salinity units, particularly in several coastal regions with strong SSS variability (Fig. 4a). The values of ε_{rms} can be attributed to a long list of both satellite and in situ observational errors, including residual calibration errors and other unresolved systematic errors (e.g., Grodsky and Carton 2012). For *Aquarius*, in addition to measurement error for the satellite sensors, which can range from 0.1 to >1 psu (Lagerloef and Delcroix 2001), other uncertainties can be related to temporal aliasing, particularly near the Amazon and Congo River outflows and in the Bay of Bengal, where aliasing noise can be >0.1 psu (Vinogradova and Ponte 2012). Aliasing can also contribute to the uncertainty of the monthly average Argo-based estimates. Other components of Argo sampling errors can

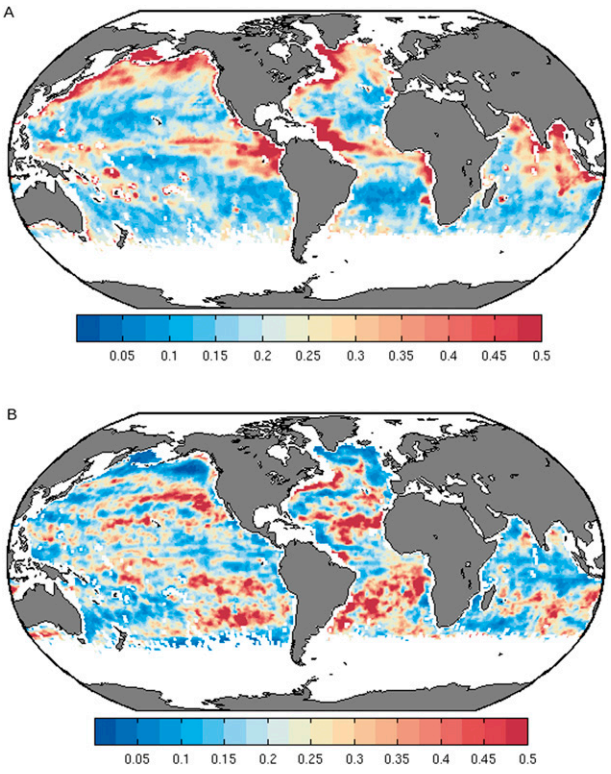

FIG. 4. Assessment of the relevance of ε_{sm} in the context of overall differences between satellite and in situ salinity data. (a) Root-mean-square difference ε_{rms} between monthly *Aquarius* and Argo-based salinity data during the period of interest. Argo grids are produced by the IPRC using variational interpolation. *Aquarius* retrievals are based on level 3, version 2.0 data provided by PO.DAAC. *Aquarius* salinity values during high-wind events ($>20\,m\,s^{-1}$) and in regions south of 45°S are not examined. (b) The ratio of $\varepsilon_{sm}/\varepsilon_{rms}$. For consistency the values of ε_{sm} in the ratio are recomputed using HYCOM monthly averaged fields, computed from daily values. Large ratio values indicate potential regions where short-scale noise can affect the comparison between *Aquarius* and Argo salinity estimates.

be related to near-surface stratification, particularly in the ITCZ (e.g., Reverdin et al. 2012; Boutin et al. 2013) and Bay of Bengal regions (e.g., Neetu et al. 2012) in Fig. 4a. We note that ε_{rms} in Fig. 4a are meant to provide an order of magnitude of the overall differences between the satellite and in situ observations. For more detailed validation analysis and definition of the *Aquarius* data errors, please see Lagerloef et al. (2013).

To examine ε_{sm} in the context of the overall differences between the satellite and in situ measurements, we compute the ratio $r_{sm} = \varepsilon_{sm}/\varepsilon_{rms}$, which can be used as an indicator of where ε_{sm} can affect validation efforts (Fig. 4b). For consistency, the values of ε_{sm} are recomputed using HYCOM monthly averaged values. Global-average value of r_{sm} is 0.2, but r_{sm} can attain values near 0.5 and above. Therefore, small-scale variability could become an important source of sampling error for the in situ measurements. As was noted above, the values in Fig. 4b can depend on the definition of ε_{rms}. For example, Boutin et al. (2013) demonstrate that the differences (biases) between the satellite and in situ measurements are typically smaller when one considers individual measurements rather than gridded analysis, which can include errors related to smoothing algorithms. One reviewer actually computed the root-mean-square difference between a single Argo measurement and corresponding Argo-gridded estimate over years 2010 and 2011, showing values exceeding 0.5 psu in frontal regions, similar to the analysis by Boutin et al. (2013), which is based on a 3-month period. Thus, the values of r_{sm} in Fig. 4b may be underestimated and the relevance of small-scale noise might increase when one considers individual in situ measurements, rather than gridded analysis.

5. Conclusions

Based on a solution from a global high-resolution HYCOM data assimilation system, the expected root-mean-square difference between in situ and satellite SSS measurements in the presence of small-scale variability ε_{sm} is <0.1 psu in most of the ocean (global median is 0.05 psu). However, local values can be significantly higher and $\varepsilon_{sm} > 0.2$ psu, particularly near strong currents and near the outflows of major rivers. In these regions, sampling error related to small-scale noise greatly exceeds in situ instrument noise and becomes an important source of observational error for in situ data.

We note that because of the limited horizontal resolution in HYCOM, spatial variations at scales $<1/12°$ are not included in the present analysis. Therefore, HYCOM-based estimates might underestimate the effects of σ_{sm} and the impact of ε_{sm} could be larger when actual ''local'' measurements are considered. More generally, the quality of the HYCOM estimates can be affected by poor data coverage, inadequate model parameterizations, unresolved variability (including near-surface gradients), and other data and model uncertainties. For example, some uncertainties in HYCOM surface salinity can be due to relaxation of monthly climatology, which might affect salinity variations at nonseasonal time scales. More details on the HYCOM solution can be found in Metzger et al. (2008a,b). Analysis of small-scale noise using other assimilation products will be helpful in the future. We also note that the results here are based on a relatively short time period and the analyses of a multiyear period would be useful to examine

the effects of σ_{sm} on longer time scales, as well as to test the robustness of our conclusions for the seasonal cycle.

In *Aquarius* calibration/validation efforts, the values of ε_{sm} can be used as a guide for a lower bound on the expected difference between the local (in situ) and averaged (satellite) quantities. Alternatively, ε_{sm} can be considered as an additional in situ measurement error, in a root-sum-square sense. Following our methodology, similar maps of ε_{sm} can be derived for the calibration/validation of the *SMOS* satellite data. Notice, however, that the *SMOS* footprint is geometrically different from the *Aquarius* footprint, with a mean spatial resolution of approximately 40 km. Therefore, corresponding adjustments are required when constructing coarse grids from the HYCOM original high-resolution fields.

Estimates of ε_{sm} will also be useful when merging in situ measurements with *Aquarius* and *SMOS* data to produce first level 4 observational SSS products. Given the difference in sampling characteristics of each platform, inclusion of ε_{sm} is essential for appropriate weighting of the data, along with other uncertainties related to temporal variability, averaging errors, etc. The regions where the impact of σ_{sm} is the highest, including the tropics and western boundary current regions, are also those that are affected by significant aliasing noise because of unresolved temporal variability (Vinogradova and Ponte 2012). In such regions, considering errors related to both of these effects as an additional source of uncertainty seems particularly relevant.

Acknowledgments. This work was supported by NASA's Physical Oceanography Program and the Ocean Surface Salinity Project through Contract NNH10CC10C to AER. We thank five anonymous reviewers, who helped us improve our manuscript, including pointing out an error in our previous analysis.

REFERENCES

Boutin, J., N. Martin, G. Reverdin, X. Yin, and F. Gaillard, 2013: Sea surface freshening inferred from *SMOS* and ARGO salinity: Impact of rain. *Ocean Sci.,* **9,** 183–192, doi:10.5194/os-9-183-2013.

Chassignet, E. P., and Coauthors, 2009: US GODAE: Global ocean prediction with the Hybrid Coordinate Ocean Model (HYCOM). *Oceanography,* **22** (2), 64–75, doi:10.5670/oceanog.2009.39.

Cummings, J. A., 2005: Operational multivariate ocean data assimilation. *Quart. J. Roy. Meteor. Soc.,* **131,** 3583–3604, doi:10.1256/qj.05.105.

Delcroix, T. M., J. McPhaden, A. Dessier, and Y. Gouriou, 2005: Time and space scales for sea surface salinity in the tropical oceans. *Deep-Sea Res.,* **52,** 787–813.

Ebuchi, N., and H. Abe, 2012: Evaluation of sea surface salinity observed by Aquarius. *Proc. IEEE Int. Geoscience and Remote Sensing Symp.,* Munich, Germany, IEEE, Paper 2246.

Emery, W. J., and R. E. Thomson, 2004: *Data Analysis in Physical Oceanography.* Elsevier, 638 pp.

Font, J., and Coauthors, 2010: *SMOS*: The challenging sea surface salinity measurement from space. *Proc. IEEE,* **98,** 649–665.

Fox, D. N., W. J. Teague, C. N. Barron, M. R. Carnes, and C. Lee, 2002: The Modular Ocean Data Assimilation System (MODAS). *J. Atmos. Oceanic Technol.,* **19,** 240–252.

Grodsky, S. A., and J. A. Carton, 2012: Accuracy of Aquarius/SAC-D sea surface salinity. PODAAC, 21 pp. [Available online at http://podaac.jpl.nasa.gov/forum/sites/default/files/SSS_AQ_buoy_JC.pdf.]

Hénin, C., and J. Grelet, 1996: A merchant ship thermosalinograph network in the Pacific Ocean. *Deep-Sea Res.,* **43,** 1833–1856.

Kaplan, A., 2009: Small-scale variability and observational error estimates for gridded analyses of sea surface temperature data. *Proc. GHRSST X Science Team Meeting,* Santa Rosa, CA, Group for High Resolution Sea Surface Temperature. [Available online at https://www.ghrsst.org/files/download.php?m=documents&f=KAPLAN-SST-Variability-and-analysis.ppt.]

Lagerloef, G., 2012: Satellite mission monitors ocean surface salinity. *Eos, Trans. Amer. Geophys. Union,* **93,** 233–234, doi:10.1029/2012EO250001.

——, and T. Delcroix, 2001: Sea surface salinity; a regional case study for the tropical Pacific. *Observing the Oceans in the 21st Century: A Strategy for Global Observations,* C. Koblinsky and N. Smith, Eds., GODAE Project Office, Bureau of Meteorology, Melbourne, Australia, 137–148.

——, and Coauthors, 2008: The Aquarius/SAC-D mission: Designed to meet the salinity remote-sensing challenge. *Oceanography,* **21** (1), 68–81.

——, and Coauthors, 2010: Resolving the global surface salinity field and variations by integrating satellite and in situ observations. *Proceedings of OceanObs'09: Sustained Ocean Observations and Information for Society,* J. Hall, D. Harrison, and D. Stammer, Eds., Vol. 2, ESA Publ. WPP-306, doi:10.5270/OceanObs09.cwp.51.

——, and Coauthors, 2013: Aquarius salinity validation analysis. Data version 2.0, Aquarius Tech. Rep. AQ-014-PS-0016, PODAAC, 36 pp. [Available online at http://aquarius.nasa.gov/pdfs/AQ-014-PS-0016_AquariusSalinityDataValidationAnalysis_DatasetVersion2.0.pdf.]

Le Vine, D. M., G. S. E. Lagerloef, F. R. Colomb, S. H. Yueh, and F. A. Pellerano, 2007: Aquarius: An instrument to monitor sea surface salinity from space. *IEEE Trans. Geosci. Remote Sens.,* **45,** 2040–2050.

Metzger, E. J., O. M. Smedstad, P. Thoppil, H. E. Hurlburt, A. J. Wallcraft, D. S. Franklin, J. F. Shriver, and L. F. Smedstad, 2008a: Validation test report for the Global Ocean Prediction System v3.0—1/12° HYCOM/NCODA: Phase I. NRL Tech. Rep. NRL/MR/7320–08–9148, 88 pp.

——, and Coauthors, 2008b: Validation test report for the Global Ocean Prediction System v3.0—1/12° HYCOM/NCODA: Phase II. NRL Tech. Rep. NRL/MR/7320–10–9236, 70 pp.

Neetu, S., M. Lengaigne, E. M. Vincent, J. Vialard, G. Madec, G. Samson, M. R. Ramesh Kumar, and F. Durand, 2012: Influence of upper-ocean stratification on tropical cyclone-induced surface cooling in the Bay of Bengal. *J. Geophys. Res.,* **117,** C12020, doi:10.1029/2012JC008433.

Reverdin, G., S. Morisset, J. Boutin, and N. Martin, 2012: Rain-induced variability of near-surface T and S from drifter data. *J. Geophys. Res.,* **117,** C02032, doi:10.1029/2011JC007549.

Vinogradova, N. T., and R. M. Ponte, 2012: Assessing temporal aliasing in satellite-based surface salinity measurements. *J. Atmos. Oceanic Technol.,* **29,** 1391–1400.